Role of spin effects in $^{12}C(^{6}\vec{Li},d)^{16}O_{g.s.}$

T. L. Drummer, E. E. Bartosz, P. D. Cathers, M. Fauerbach, K. W. Kemper, and E. G. Myers
Department of Physics, Florida State University, Tallahassee, Florida 32306-4350

K. Rusek
The A. Soltan Institute for Nuclear Studies, Warsaw, Poland

(Received 27 May 1998)

The first complete set of analyzing powers for the $^{12}C(^{6}\vec{Li},d)^{16}O_{g.s.}$ reaction at $E(^{6}Li)=50$ MeV is reported. It was possible to simultaneously describe $^{6}Li+^{12}C$ elastic scattering and its analyzing powers, $d+^{16}O$ elastic scattering, and the $^{12}C(^{6}\vec{Li},d)^{16}O_{g.s.}$ transfer data. This $0^{+}\rightarrow 0^{+}$ transfer is used to probe the role of spin-dependent interactions in this reaction, including the ^{6}Li D state, with finite-range-distorted-wave-Born-approximation calculations. It is found that the exit channel spin-orbit $d+^{16}O$ interaction produces the transfer analyzing powers, but that the shape and magnitude of the transfer angular distribution is determined by the central $^{6}Li+^{12}C$ and $d+^{16}O$ interactions. The limited knowledge of the size of the $\alpha+^{12}C$ system is shown to be the major uncertainty in using the $^{12}C(^{6}Li,d)^{16}O$ reaction to determine absolute $\alpha+^{12}C$ spectroscopic factors. [S0556-2813(99)00605-6]

PACS number(s): 21.10.Jx, 21.60.Gx, 25.45.De, 25.70.Hi

For several decades there has been a great deal of interest in the α-clustering strength of states in ^{16}O [1]. Recent studies to determine the $^{12}C/^{16}O$ ratio in the late stage stellar evolution of massive stars has rekindled interest in α-cluster transfer reactions as a probe of α clustering [2] in light nuclei. One reaction that was proposed almost 30 years ago [3] to probe the α structure of ^{16}O was the $^{12}C(^{6}Li,d)^{16}O$ reaction. There have been many measurements of the $^{12}C(^{6}Li,d)^{16}O$ cross section at different energies and numerous analyses have been performed to extract α spectroscopic factors for states in ^{16}O [4–8]. In general, previous analyses were not able to simultaneously describe the entrance and exit channel elastic scattering and transfer cross sections [4,5] so that it was not possible to resolve the model dependent ambiguities that arise from the large angular momentum mismatch occurring in this reaction [5,6]. In the present work, all available ^{6}Li and d elastic scattering scattering data for the present ^{6}Li bombarding energy of 50 MeV are described as well as the new $(^{6}\vec{Li},d)$ transfer angular distribution and analyzing power data.

The present work reports the first complete set of analyzing powers that has been measured for the $^{12}C(^{6}Li,d)$ reaction. An early measurement of the $^{12}C(^{6}Li,d)^{16}O$ vector analyzing power (iT_{11}) for $E(^{6}Li)=20$ MeV showed this analyzing power to be large [9], suggesting that analyzing powers could be useful in gaining an understanding of the $(^{6}Li,d)$ reaction. In addition to the complete set of analyzing powers, the $^{12}C(^{6}Li,d)$ cross section has also been measured. The present data, taken at a ^{6}Li bombarding energy of 50 MeV, makes use of the $0^{+}\rightarrow 0^{+}$, ^{12}C(g.s.) to ^{16}O(g.s.) reaction to explore in detail the results of numerous model assumptions that have been made in previous works. The ground state $0^{+}\rightarrow 0^{+}$ transfer provides an excellent laboratory for the testing of the role played by spin-dependent potentials in the model calculations since it can have no preferred orientation in space, so that the observed analyzing powers, which are large and highly oscillatory, can only arise through spin-dependent distortions. The present greatly expanded data set was compared to finite-range-distorted-wave-Born-approximation calculations (FRDWBA) to determine the origin of the observed analyzing powers and the dependence of the magnitude of the ground state α spectroscopic factor on the model assumptions commonly made for this reaction.

A beam of polarized ^{6}Li nuclei was produced by the Florida State University (FSU) Optically Pumped Polarized Lithium Ion Source [10]. The polarized beam was accelerated with the FSU FN tandem Van de Graaff/Superconducting Linear Accelerator to 50 MeV. The ^{12}C target was self-supporting of thickness 500 $\mu g/cm^{2}$. Four Si surface-barrier detectors were arranged in two ΔE-E telescope configurations, placed symmetrically on either side of the incident beam. The telescopes had an angular acceptance of $\pm 0.83°$. Thin tantalum foils were placed in front of each detector during the analyzing power measurements to prevent the huge flux of elastically scattered ^{6}Li ions from striking the detectors. The beam polarization was monitored using a helium-filled polarimeter which followed the main chamber and was separated from it via a thin Havar window. The ^{6}Li nucleus has spin 1, and therefore has the three magnetic substates of $m_I=+1$, 0, and -1. During the experiment, the polarization state of the beam was cycled through the off, N_{+}, N_{0}, and N_{-} states approximately every 2 min. The on-target vector polarization was found to be $|t_{10}|=0.98\pm 0.05$ and the tensor polarization was found to be $t_{20}=-1.10\pm 0.05$ with typical beam currents of 150–200 enA. The polarization observables are described in terms of the Madison convention [11]. The angular distribution data were taken using an unpolarized ^{6}Li beam from the laboratory's sputter source. An absolute cross section was obtained by removing the tantalum foils from the ΔE-E telescopes so that $^{6}Li+^{12}C$ elastic scattering could be measured simultaneously with the $(^{6}Li,d)$ data. The previously measured absolute elastic cross section was then used to provide a nor-

 ©1999 The American Physical Society

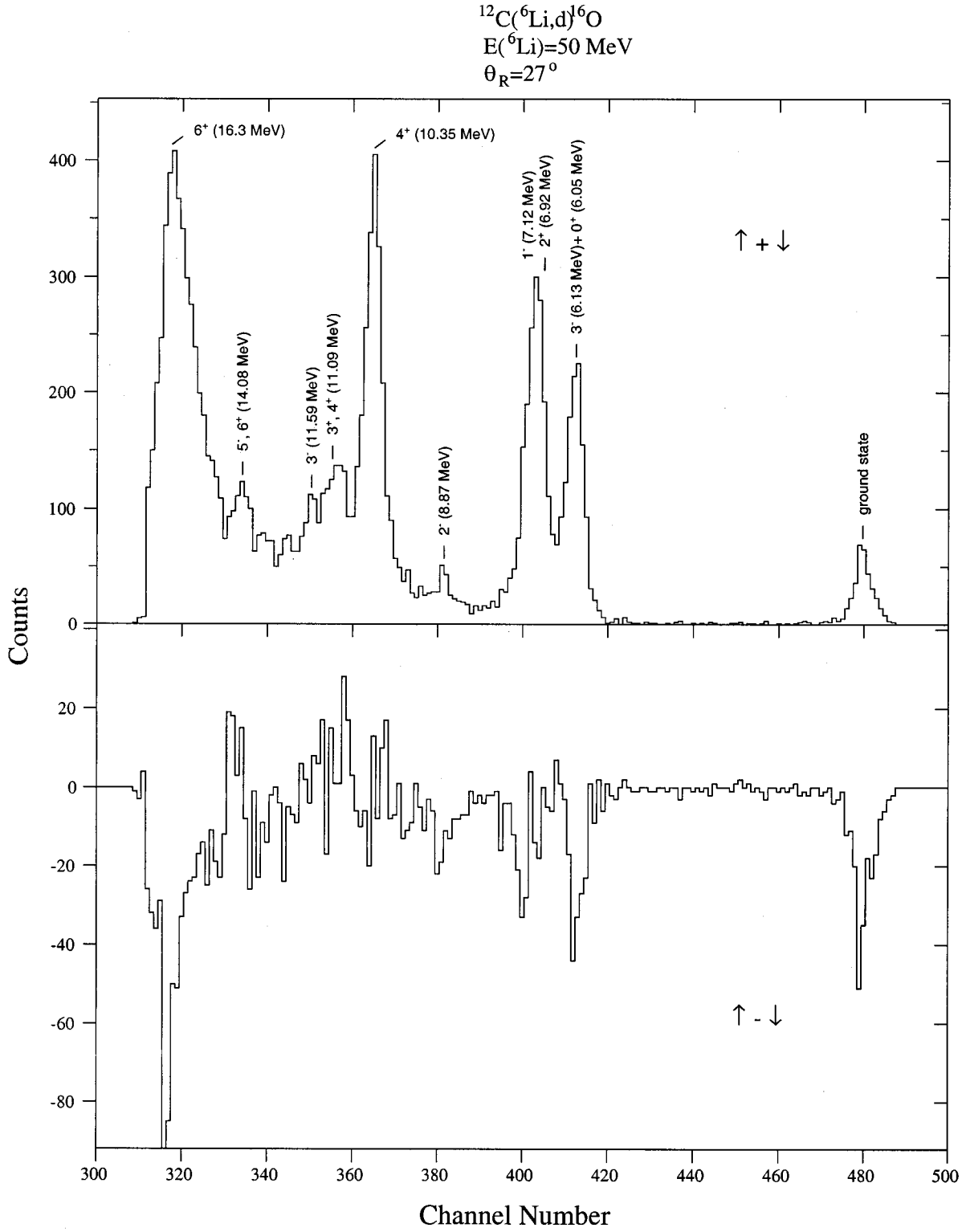

FIG. 1. A typical spectrum for the $^{12}C(^6Li,d)^{16}O$ reaction measured in the present work. The top portion of the figure adds the data taken with the projectile spin up and down so that it is a cross section spectrum. In the bottom portion of the figure, the spin up data are subtracted from the spin down data so that the figure is a measure of the reaction vector analyzing power.

malization factor to connect the $^{12}C(^6Li,d)$ angular distribution to the absolute cross section elastic scattering data. The error in the absolute cross section was $\pm 15\%$ and arose primarily from the spread in the normalization factors at the various angles and the reproducibility of the angle setting for the rapidly oscillating elastic scattering. The ground state cross section magnitude measured in this manner compared well with the cross section measurements of Cunsolo *et al.* [4], at 34 MeV and Becchetti *et al.* [5], at 42 MeV. Figure 1 shows a typical spectrum with the upper part being the unpolarized cross section and the lower part showing the vector analyzing power at the laboratory angle of

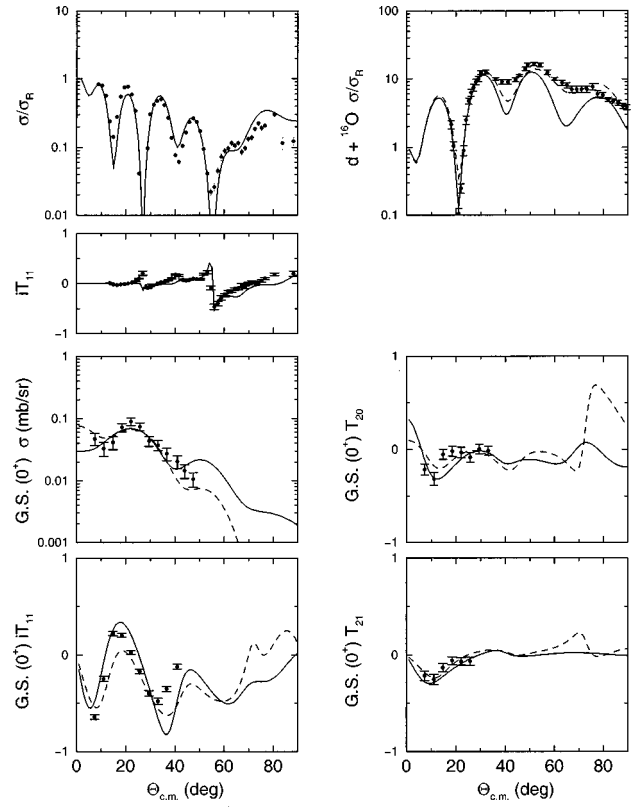

FIG. 2. FRDWBA calculations for α transfer to the ^{16}O ground state at 50 MeV. The solid line corresponds to calculations with an ^{16}O bound state radius of $R=3.07$ fm and the dashed line corresponds to calculations with an ^{16}O bound state radius of $R=4.85$ fm. The top three panels are the ^{6}Li+^{12}C elastic scattering data of Kerr *et al.* [12] and the $d+^{16}$O elastic scattering data of Hinterberger *et al.* [13] and their corresponding optical model descriptions.

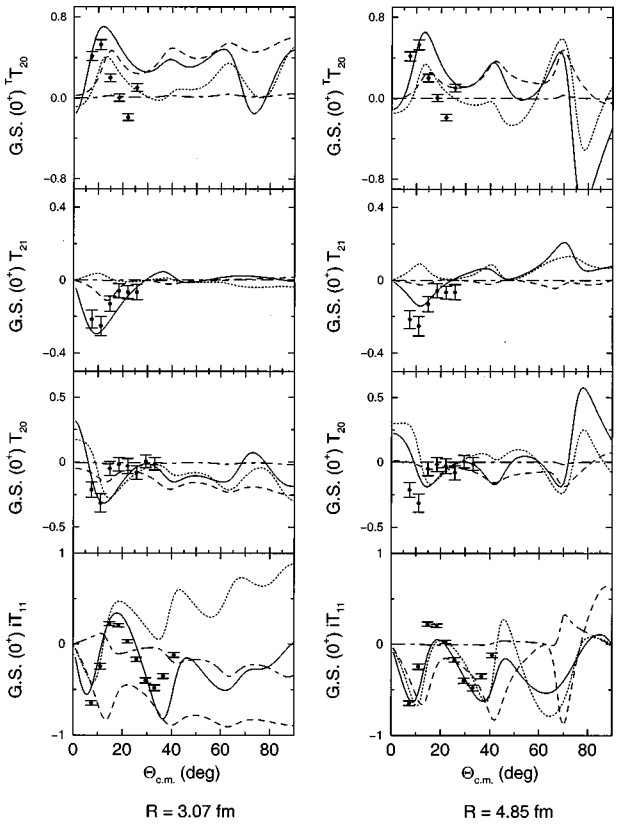

FIG. 3. Effects of the deuteron spin-orbit potential on the ^{12}C(^{6}Li,d)^{16}O calculations. The solid line is a calculation with the full deuteron spin-orbit potential, the dashed line is with the imaginary deuteron spin-orbit potential only, the dotted line is with the real spin-orbit potential only, and the dot-dashed line is with no deuteron spin-orbit potential. In all calculations, the ^{6}Li spin-orbit potential was included.

27°. Figure 2 shows the angular distribution and analyzing power data. The errors shown in Fig. 2 for the ^{12}C($^{6}\vec{\text{Li}}$,d) data are purely statistical.

The information needed to perform FRDWBA calculations were entrance (^{6}Li+^{12}C) and exit ($d+^{16}$O) channel optical model parameters from which the distorted waves were generated, and $^{6}\text{Li}\rightarrow\alpha+d$ and $^{16}\text{O}\rightarrow\alpha+^{12}$C bound state wave functions. The ^{6}Li bombarding energy of 50 MeV was chosen for this work because extensive $^{6}\vec{\text{Li}}+^{12}$C elastic scattering analyzing power data already exists which severely constrains the choice of distorting potentials and similarly $d+^{16}$O elastic scattering data at energies close to that needed for the present work, 44 MeV, are also available [13,14]. Detailed polarized $d+^{16}$O scattering measurements also exist at the energies of 52 [15] and 56 MeV [16] which serve as an additional constraint on the deuteron optical potentials. The present ^{6}Li bombarding energy has the advantage over previous lower ^{6}Li energy studies in that the experimental characteristics of the deuteron scattering and analyzing power angular distributions [17] are stable beginning around the deuteron energy of the present work (44 MeV) up to 80 MeV, so that it is possible to assess the importance of the $d+^{16}$O exit channel in the transfer process by comparing the transfer analyzing powers with those measured previously for $d+^{16}$O elastic scattering. Perhaps one of the most dramatic similarities in the present data set and that for $d+^{16}$O is the rapid oscillation in $^{T}T_{20}$ shown in Fig. 3, which also occurs in the deuteron scattering data [16].

The ^{6}Li bound state wave function was generated by assuming $\alpha+d$ clusters in a relative S state with the α particle bound in a Woods-Saxon potential well. Investigation of the effect of the D state of ^{6}Li on the transfer reaction is discussed in a later section. The quantum numbers for the $\alpha+d$ system were assumed to be $2N+L=2$. The potential geometry was chosen such that the radius agreed with a detailed three-body calculation performed by Lehman and Rajan [18], corresponding to a potential radius of $R=2.39$ fm. This value also agrees with the one determined by Kubo and Hirata [19], who examined the validity of the DWBA method for studying alpha transfer reactions. The bound state geometry of the $\alpha+^{12}$C system was not as straightforward. There is an ongoing discussion in the literature regarding the correct bound state radius. Many ^{12}C(^{6}Li,d) studies have chosen a radius for the $\alpha+^{12}$C system which agrees with the results of elastic electron scattering, namely, $R=3.07$ fm, while others have cited the constancy of the nuclear density and chosen a bound state radius which agrees with the value obtained from $R=1.25(A_{\text{alpha}}^{1/3}+A_{\text{carbon}}^{1/3})=4.85$ fm. As a result, both values were adopted in the present analysis.

The first set of DWBA calculations were performed to determine whether the $^{6}\vec{\text{Li}}+^{12}$C spin-orbit potential found

from elastic scattering studies could produce the large transfer analyzing powers observed in $^{12}C(\vec{^6Li},d)^{16}O$. The entrance channel optical parameters were based on those found in a global analysis of $^6Li+^{12}C$ elastic scattering by Vineyard *et al.* [20], adjusted to fit the 50 MeV elastic scattering by increasing the imaginary potential strength. The ^6Li spin-orbit potential was from a study by Kemper *et al.* [21], where the final state J dependence of the reaction $^{12}C(\vec{^6Li},^3He)$ at 34 MeV was investigated. As can be seen in Fig. 2, this spin-orbit potential gave an excellent account of the 50 MeV elastic vector analyzing power without any modification. The $d+^{16}O$ potentials for generating these distorted waves were taken from the 34 MeV $d+^{16}O$ elastic scattering study of Newman *et al.* [14]. This parameter set does not contain a $d+^{16}O$ spin-orbit interaction but gave a very good description of the elastic cross section data. It was found that no adjustment of the $^6Li+^{12}C$ entrance channel potentials which was still consistent with the elastic scattering data could yield the large transfer analyzing powers. This result implies that the transfer analyzing powers arise from the outgoing $d+^{16}O$ interaction so that further efforts to describe the transfer data concentrated on the $d+^{16}O$ interaction potentials. The rapidly changing shapes of the $(^6Li,d)$ analyzing powers and the similarity of their shapes and magnitudes with those of Matsuoka *et al.* [16] for $d+^{16}O$ at 56 MeV, further suggests that the $d+^{16}O$ final state spin effects are responsible for the $(^6Li,d)$ analyzing powers. In particular, the very strong deuteron spin-orbit interaction is known [17,22] to dominate the $d+^{16}O$ analyzing powers in this energy region and so it is anticipated from the data alone that it should be responsible for the $(^6Li,d)$ analyzing powers.

The $d+^{16}O$ spin-dependent interactions considered in the present work were based on the deuteron potentials of Matsuoka *et al.* [16], for elastic scattering at $E(d)=56$ MeV. These parameters included both surface and volume absorption terms, and a real deuteron spin-orbit potential; however, calculations using these potentials also failed to describe the transfer angular distribution and analyzing powers. Starting from the Matsuoka parameters, adjustments were then made to the deuteron potentials to achieve a good description of the transfer data, while always maintaining the fit to the elastic scattering data. It was found that by retaining both a surface and a volume absorption potential in the exit channel optical potentials, and adding an imaginary spin-orbit term, that the transfer angular distributions could be well described for both the smaller and the larger ^{16}O bound state radii. The only difference in the optical potentials was that the real and imaginary spin-orbit strengths and imaginary absorptive potential radius was larger at 4.85 fm. The inclusion of an imaginary spin-orbit potential was shown by Goddard and Haeberli [23] to significantly improve the optical model description of precise deuteron elastic scattering vector analyzing power data.

The determination of a satisfactory $d+^{16}O$ potential set required several hundred FRDWBA calculations. The results are shown in Fig. 2. The final $^6Li+^{12}C$ optical potentials were the same as Vineyard's set III, except the imaginary volume strength was increased to 10 MeV: $V_R=186.0$ MeV, $r_R=1.13$ fm, $a_R=0.83$ fm, $W_V=10.0$ MeV, $r_V=2.26$, and $a_V=0.62$ fm. The ^6Li spin-orbit was $V_{SO}=2.0$ MeV, $r_{SO}=1.16$ fm, and $a_{SO}=0.39$ fm. The final $d+^{16}O$ parameters were as follows: $V_R=89.3$ MeV, $r_R=0.99$ fm, $a_R=0.95$ fm, $W_V=7.3$ MeV, $r_V=2.10$ fm, $a_V=0.30$, $W_S=3.125$ MeV, $r_S=2.25$ fm, and $a_S=0.30$ fm. The deuteron spin-orbit real potential was $V_{SO}=9.0$ (15.0) MeV, $r_{SO}=0.90$ fm, $a_{SO}=0.27$ fm, and the imaginary spin-orbit potential was $W_{SO}=7.0$ (9.0) MeV, $r_{SO}=1.15$ (1.60) fm, and $a_{SO}=0.35$ fm. The values in parentheses correspond to the larger ^{16}O bound state radius values. The form factors for the optical potentials were the same as those in Ref. [16]. The final calculations and data are shown in Fig. 2.

Once the best description of the ground state α transfer data had been achieved, it was natural to inquire into the origin of the observed analyzing powers. The role of the deuteron spin-orbit potential was investigated first. Calculations were performed with only a real deuteron spin-orbit potential, only an imaginary deuteron spin-orbit potential, and without deuteron spin-orbit terms, always including the ^6Li spin-orbit potential. As can be seen in Fig. 3, without a deuteron spin-orbit potential, no tensor analyzing powers appear and only minimal effects in the calculated vector analyzing power were observed. There was a dependence of the deuteron spin-orbit on the bound state radius of ^{16}O and this was seen in the specific contributions of the real and imaginary spin-orbit potential terms at the two separate radii. For the $R=3.07$ fm calculations, the imaginary spin-orbit contribution was negative everywhere while the real spin-orbit contribution is positive, and the sum of the two contributions added to form the correct shape to describe the measured data. The larger radius calculations show that both the real and imaginary deuteron spin-orbit contributions were of nearly the same magnitude and phase. Note that the second order spin-orbit effects were able to reproduce the tensor analyzing powers for both bound state radii.

The tensor analyzing powers are normally used to probe ^6Li D-state and tensor potential effects, and even though the tensor analyzing powers are well described by the deuteron spin-orbit potential, calculations were performed to investigate their effects on the calculated tensor analyzing powers. The $^6Li+^{12}C$ tensor interaction was based on the work done by Reber *et al.* [24], who investigated the importance of spin-orbit and tensor potentials from polarized ^6Li elastic scattering at a bombarding energy of 30 MeV. The Raynal tensor form factor [25] was used to describe the radial part of both the real and imaginary tensor potentials. The geometries for the real and imaginary $^6Li+^{12}C$ tensor potential were taken from Ref. [24].

The $d+^{16}O$ tensor potential was taken from the work of Frick *et al.* [26], where the deuteron tensor potential was examined by studying its effect on the calculated elastic scattering cross sections and analyzing powers for 20 MeV deuterons. For the real and imaginary potentials, Frick *et al.* used radial forms similar to those found by Keaton and Armstrong [27] who derived analytic expressions to describe the deuteron potential arising from the static folding model. The real and imaginary deuteron central potentials have individual geometries whose values were taken from Frick *et al.* An imaginary volume Woods-Saxon term was added to the imaginary deuteron tensor potential by Frick *et al.* because it resulted in a substantial improvement in their description of

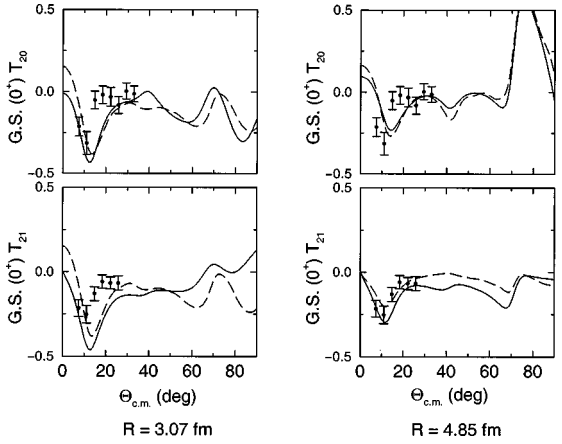

FIG. 4. Effects of including ^{6}Li+^{12}C and $d+^{16}$O tensor potentials on the FRDWBA calculations. The solid line is for calculations with the tensor potentials and the dashed line is for calculations without the tensor potentials.

the $d+^{16}$O data, so it was included here as well. The tensor potential spin coupling was of the T_R type as discussed by Satchler [28]. As can be seen in Fig. 4, including tensor potentials in the DWBA calculations did not improve the quality of the fit to the tensor analyzing power data, and actually degraded the fit slightly. The small role played by the ^{6}Li tensor force in producing the (^{6}Li,d) analyzing powers is further evidence for the dominance of the $d+^{16}$O spin orbit potential in producing the transfer tensor analyzing powers. The analysis of $d+^{16}$O tensor analyzing powers [17,22] show that they are dominated by second order spin-orbit effects as are the present transfer analyzing powers.

It is known that the ^{6}Li wave function has a small ($\leqslant 4\%$) D-state component [29] in its wave function and therefore calculations were performed to examine the contribution of the D state to the description of the ground state α transfer tensor analyzing powers. Including a D-state component increased the number of L transfers that can occur in the α transfer reaction. D-state spectroscopic amplitudes ranging from -0.20 to $+0.20$ were examined. It was found that values of the D-state spectroscopic amplitude greater in magnitude than 0.10 resulted in a substantially worse description of the data, while smaller values did not improve the description of the tensor analyzing power data. Hence, the D-state component does not contribute to the ^{12}C(^{6}Li,d) reaction. The small role played by the ^{6}Li D-state in the (^{6}Li,d) reaction observed in the present work has also been reported for the (^{6}Li,d) reaction on medium-weight nuclei (Ca,Ni) by Veal *et al.* [30].

α particle spectroscopic factors were extracted from the ground state transfer calculations by normalizing the theoretical cross sections to the measured cross section. The values obtained are given in Table I along with values from Cunsolo *et al.* [4] and Becchetti *et al.* [5,6]. The quantity needed for astrophysical calculations is the α reduced width and so its values were also extracted and are given in Table I. The formalism used for extracting the α reduced width is given by Becchetti *et al.* [5]. The channel radius used in the present work for determining the α reduced width was the radius at which the ^{12}C+α binding potential had decreased to 10% of its largest value, which for the $R=3.07$ fm calculations corresponds to a channel radius of 5.4 fm and for the $R=4.85$ fm calculation, the channel radius was 7.20 fm. In the works of Becchetti *et al.*, a channel radius of 5.4 fm was used. The radius for the $\alpha+^{12}$C system, of interest to the astrophysical ^{12}C/^{16}O abundance question is typically taken to be 5.5 fm [31]. Redder *et al.* [31] used the many-level R-matrix formalism of nuclear reactions to analyze $E1$ and $E2$ ^{12}C(α,γ) capture data. They concluded that the appropriate channel radius for α capture was 5.5 fm, and at this radius the ground state reduced width was 0.012 ± 0.012, well below our value of 0.44 for the same channel radius.

In summary, a FRDWBA calculation using a standard optical model parametrization of the entrance and exit channel interactions gave an excellent simultaneous description of ^{6}Li+^{12}C and $d+^{16}$O elastic scattering and the ^{12}C(^{6}Li,d)^{16}O reaction at 50 MeV. No adjustment of the ^{6}Li+^{12}C potentials could generate the large observed transfer analyzing powers, as long as the fit to the ^{6}Li+^{12}C elastic scattering data was maintained whereas they occured quite naturally when the deuteron spin-orbit potential was added. The inclusion of the D-state component of the ^{6}Li wave function, worsened the description of the data, indicating that the reaction was predominantly S-wave transfer.

The extracted α particle spectroscopic factor was dominated by the spin-independent potentials, changing by less than 20% for calculations with and without the deuteron spin

TABLE I. Summary of the extracted α spectroscopic factors and α reduced widths.

Quantity	Current 50 MeV $R^a=3.07$ fm	Current 50 MeV $R^a=4.85$ fm	Cunsolo [4] 28 MeV $R^a=4.85$ fm	Becchetti [5] 42 MeV $R^a=2.98$ fm	Becchetti [6] 90 MeV $R^a=2.98$ fm
Spectroscopic Factor	14.29	0.32	0.23 [b]	14.3 [b]	11.08 [b]
Dimensionless Reduced Widths	0.44(5.40) [c]	0.0044(7.20) [c]		0.75(5.40) [c]	0.29(5.40) [c]

[a]The ^{16}O bound state radius used in the respective calculation.

[b]These authors assumed a ^{6}Li$\rightarrow\alpha+d$ spectroscopic factor of 1.0. For comparison to the current work, this value was replaced by 0.70 from Werby *et al.* [26].

[c]The numbers in parentheses are the channel radii in fm used for determining the dimensionless reduced widths. Here, the definition of the dimensionless reduced width is taken from [5] and is given by $\Theta^2_\alpha(s)=\gamma^2_\alpha(s)/\gamma^2_w(s)$ where s is the channel radius, γ^2_α is the reduced α width, and γ_w is the single-particle Wigner limit.

orbit potential. It was seen that the ^{16}O bound state radius played a crucial role in the value of the extracted spectroscopic factors and reduced widths. The extreme range of absolute α spectroscoptic factors and hence reduced α widths found in the present work makes it extremely doubtful that the $^{12}C(^6Li,d)$ reaction can be used to extract meaningful $\alpha+^{12}C$ spectroscopic information even when a very complete data set including spin-dependent observables exists. The rather large angular momentum mismatch ($1 \approx 5\hbar$) of the reaction makes the calculation extremely sensitive to the $\alpha + ^{12}C$ wave function at large distances, where it is most difficult to determine its magnitude. As has been shown in previous works [32], it is possible that the better angular momentum matched reaction $^{12}C(^7Li,t)$ is the most reliable α transfer reaction for determining the absolute subthreshold reduced α widths needed for determining the $^{12}C(\alpha,\gamma)$ reaction rate in stars.

The authors wish to acknowledge extremely helpful discussions with C. Brune and D. Robson. This work was supported by the National Science Foundation, the State of Florida, and the State Committee for Scientific Research (KBN) of Poland.

[1] J. Wheeler, Phys. Rev. **52**, 1083 (1937); D. Robson, Phys. Rev. Lett. **42**, 876 (1979).
[2] L. Buchmann, R.E. Azuma, C.A. Barnes, J. Humblet, and K. Langanke, Phys. Rev. C **54**, 393 (1996).
[3] A.A. Ogloblin, in *Proceedings of the Fifth International Conference on Nuclear Reactions Induced by Heavy Ions*, Heidelbert, Germany, 1969, edited by R. Bock and W.R. Hering (North-Holland, Amsterdam, 1970).
[4] A. Cunsolo, A. Foti, G. Pappalardo, G. Raciti, and N. Saunier, Phys. Rev. C **18**, 856 (1978).
[5] F.D. Becchetti, J. Jänecke, and C.E. Thorn, Nucl. Phys. **A305**, 313 (1978).
[6] F.D. Becchetti, D. Overway, and J. Jänecke, Nucl. Phys. **A344**, 336 (1980).
[7] E.I. Dolinsky, V.V. Turovtsev, and Y. Yarmukhamedov, Phys. Lett. **33B**, 147 (1970).
[8] H.W. Fulbright, Annu. Rev. Nucl. Part. Sci. **29**, 161 (1979), and references therein.
[9] M. Makowska-Rzeszutko, P. Egelhof, D. Kassen, E. Steffens, W. Weiss, D. Fick, W. Dreves, K-I. Kubo, and T. Suzuki, Phys. Lett. **74B**, 187 (1978).
[10] E.G. Myers, A.J. Mendez, B.G. Schmidt, and K.W. Kemper, Nucl. Instrum. Methods Phys. Res. B **56/57**, 1156 (1991); E.G. Myers, A.J. Mendez, B.G. Schmidt, K.W. Kemper, P.L. Kerr, and E.L. Reber, *ibid.* **79**, 701 (1993).
[11] Madison Convention, *Polarization Phenomena in Nuclear Reactions*, edited by H.H. Barschall and W. Haeberli (University of Wisconsin Press, Madison, 1971), p. XXV.
[12] P.L. Kerr, K.W. Kemper, P.V. Green, K. Mohajeri, E.G. Myers, D. Robson, and B.G. Schmidt, Phys. Rev. C **52**, 1924 (1995).
[13] F. Hinterberger, G. Mairle, U. Schmidt-Rohr, G.J. Wagner, and P. Turek, Nucl. Phys. **A111**, 265 (1968).
[14] E. Newman, L.C. Becker, B.M. Preedom, and J.C. Hiebert, Nucl. Phys. **A100**, 225 (1967).
[15] G. Mairle, K.T. Knöpfle, H. Riedesel, G.J. Wagner, V. Bechtold, and L. Friedrich, Nucl. Phys. **A339**, 61 (1980).
[16] N. Matsuoka, H. Sakai, T. Saito, K. Hosono, M. Kondo, H. Ito, K. Hatanaka, T. Ichihara, A. Okihana, K. Imai, and K. Nisimura, Nucl. Phys. **A455**, 413 (1986).
[17] E.J. Stephenson, C.C. Foster, P. Schwandt, and D.A. Goldberg, Nucl. Phys. **A359**, 316 (1981).
[18] D.R. Lehman and M. Rajan, Phys. Rev. C **25**, 2743 (1982).
[19] K.-I. Kubo and M. Hirata, Nucl. Phys. **A187**, 186 (1972).
[20] M.F. Vineyard, J. Cook, K.W. Kemper, and N. Stephens, Phys. Rev. C **30**, 916 (1984).
[21] K.W. Kemper, P.L. Kerr, A.J. Mendez, E.G. Myers, E.L. Reber, K. Rusek, and G. Tungate, Phys. Lett. B **321**, 183 (1994).
[22] H. Nishioka and R.C. Johnson, Nucl. Phys. **A440**, 557 (1985).
[23] R.P. Goddard and W. Haeberli, Phys. Rev. Lett. **40**, 701 (1978).
[24] E.L. Reber, K.W. Kemper, P.V. Green, P.L. Kerr, A.J. Mendez, E.G. Myers, and B.G. Schmidt, Phys. Rev. C **49**, R1 (1994).
[25] J. Raynal, Phys. Lett. **7**, 281 (1963).
[26] R. Frick, H. Clement, P. Schiemenz, N. Siechert, and Sun Tsu-Hsun, Z. Phys. **319**, 133 (1984).
[27] P.W. Keaton and D.D. Armstrong, Phys. Rev. C **8**, 1692 (1973).
[28] G.R. Satchler, Nucl. Phys. **21**, 116 (1960).
[29] M.F. Werby, M.B. Greenfield, K.W. Kemper, D.L. McShan, and S. Edwards, Phys. Rev. C **8**, 105 (1973).
[30] K.D. Veal, C.R. Brune, W.H. Geist, H.J. Karwowski, E.J. Ludwig, A.J. Mendez, E.E. Bartosz, P.D. Cathers, T.L. Drummer, K.W. Kemper, A.M. Eiró, F.D. Santos, B. Kozlowska, H.J. Maier, and I.J. Thompson, Phys. Rev. Lett. **81**, 1187 (1998).
[31] A. Redder, H.W. Becker, C. Rolfs, H.P. Trautvetter, T.R. Donoghue, T.C. Rinckel, J.W. Hammer, and K. Langanke, Nucl. Phys. **A462**, 385 (1987).
[32] F.D. Becchetti, E.R. Flynn, D.L. Hanson, and J.W. Sunier, Nucl. Phys. **A305**, 293 (1978); F.D. Becchetti, M. Dowell, P.M. Lister, J.W. Jänecke, A. Nadasen, and J.S. Winfield, J. Phys. Soc. Jpn. **58**, 635 (1989).